Title
THE K+-p INTERACTION AT 455 Mev

Authors
Stubbs, Theodore F.
Bradner, Hugh
Chinowsky, William
et al.

Publication Date
1961-07-11

UCRL -9745

UNIVERSITY OF CALIFORNIA

Ernest O. Lawrence

Radiation Laboratory

BERKELEY, CALIFORNIA

DISCLAIMER

To be published in Phys. Rev. Letters

UCRL-9745

UNIVERSITY OF CALIFORNIA

Lawrence Radiation Laboratory
Berkeley, California

Contract No. W-7405-eng-48

THE K^+-p INTERACTION AT 455 Mev

Theodore F. Stubbs, Hugh Bradner, William Chinowsky,
Gerson Goldhaber and Sulamith Goldhaber

and

William Slater, Donald M. Stork, and Harold K. Ticho

July 11, 1961

THE K^+-p INTERACTION AT 455 Mev*

Theodore F. Stubbs, Hugh Bradner, William Chinowsky, Gerson Goldhaber, and Sulamith Goldhaber

Lawrence Radiation Laboratory and Department of Physics
University of California, Berkeley, California

and

William Slater, Donald M. Stork, and Harold K. Ticho

Department of Physics
University of California, Los Angeles, California

July 11, 1961

We have undertaken a systematic study of the interaction of positive K mesons with hydrogen and deuterium in the energy interval from 0 to 455 Mev. Some preliminary results have already been reported.[1] In this note we present the results obtained for the elastic and inelastic K^+-p interaction at 455 Mev.

Previous investigations of K^+ interactions in nuclear emulsion[2] and propane[3] have yielded measurements of differential and total cross sections for the process $K^+ + p \rightarrow K^+ + p$ in the energy interval 40 to 300 Mev. The differential cross section at 225 Mev,[4] as well as the total cross sections in the range 175 Mev $< E_K <$ 8 Bev, have been measured by counter techniques.[5,6] The features of the K^+-p scattering from 80 to 300 Mev are: (a) the total cross section is approximately 14 mb, varying little, if at all, with energy; and (b) the angular distribution is isotropic.

The Lawrence Radiation Laboratory 15-inch hydrogen bubble chamber was exposed to a separated beam of K^+ mesons produced by the 6-Bev circulating protons of the Bevatron (Fig. 1). The system was designed for a momentum of 645 Mev/c. With adjustment of the magnet parameters it was possible to obtain the higher momentum of 810 Mev/c ($T_K \approx$ 455 Mev). A mass-resolution curve at 810 Mev/c for the separation system is shown in Fig. 2. The background of light particles (pions, muons, and electrons) was approximately 10%; the pion component is analyzed in more detail below.

The initial sample of events, chosen to satisfy geometric and incident-momentum criteria, contained both inelastic and elastic K^+ interactions and also a background of π^+ interactions. Kinematical fitting procedure (with further evidence from estimates of bubble density of the secondary tracks) provide means of separating the elastic from inelastic interactions with essentially complete certainty. The elastic pion scatterings are distinguishable from K^+ elastic scatterings for $\cos\theta_\pi^{cm} < 0.4$. To determine the total number of pion scatterings, we use the π^+-p angular distribution[7] to evaluate the number of such events in the remaining angular interval $0.4 < \cos\theta_\pi^{c.m.} < 0.96$. This number (i.e., 31 events) is then subtracted from the group consistent with K^+-p elastic scatterings. The observed number of π^+ inelastic interactions (i.e., 29 events) is in agreement with the sum of observed and inferred numbers of π^+ elastic interactions. The contamination of pion inelastic scatterings in the sample of K^+-p elastic scatterings is thus negligible. We accepted only those scatterings with $\cos\theta_K^{c.m.} < 0.96$ in order to preclude any effects of low efficiency for detecting small-angle scattering. We find, then, a total of 1320 elastic K^+-p scatterings satisfying the above conditions. The total K^+ path length was determined by three independent methods:

(a) From K^+ decays into three charged secondaries (316 decays) and the known branching ratio,[8] $b_1 = 0.061 \pm .002$ for these decay modes; this yields a total path length of $(3.12 \pm .25) \times 10^6$ cm.

(b) From K^+ decays into one charged secondary with projected angle $\theta_{lab} > 27.5$ deg. This cutoff angle was introduced in order to avoid possible confusion with K^+-p scatterings without observable recoil. The decays included in this sample correspond to a fraction $b_2 = 0.29 \pm .01$ of all K^+ decays. A total path length of $(2.93 \pm 0.14) \times 10^6$ cm is obtained by this method.

(c) From a direct count of tracks passing through the chamber. After corrections for light-particle contamination, decays, and interactions, we obtain a total path length of[7] $(2.96 \pm .16) \times 10^6$ cm. The weighted average of the path lengths obtained by the above three methods is $L_{total} = (2.97 \pm 0.09) \times 10^6$ cm. Correcting for the scanning efficiency for elastic scattering, $\epsilon_s = 0.997$, and decays, $\epsilon_d = 0.994$, and extrapolating the angular distribution (considered as flat) to $\cos\theta_{cm} = 1.0$, we obtain the total elastic-scattering cross section, at 455 ± 5 Mev, $\sigma_{e\ell} = 13.0 \pm 0.7$ mb. This cross section contains some Coulomb effects below $\cos\theta_K^{c.m.} = 0.96$, and is to be compared with the purely nuclear cross sections as deduced from the phase-shift analyses below. The error includes the uncertainties in the path-length determinations and statistical error in the number of scatterings. For the inelastic K^+-p interactions, discussed below, we obtain a cross section $\sigma_{inel} = 1.0 \pm 0.2$ mb.

The differential cross section plotted in Fig. 3 shows only a small angular dependence. We analyzed the data in terms of s- and p-wave scattering for the elastic and inelastic interaction.

We can thus write the differential cross section as

$$\left(\frac{d\sigma}{d\Omega}\right)_{e\ell} = \frac{1}{4k^2}\left\{\left|\frac{-i\alpha}{\sin^2\theta/2}\exp(-i\alpha\ell n\sin^2\theta/2) + \eta_1 e^{2i\delta_1} - 1 + \frac{1+i\alpha}{1-i\alpha}\left(\eta_{11}e^{2i\delta_{11}} + 2\eta_{13}e^{2i\delta_{13}} - 3\right)\cos\theta\right|^2 + \left|\eta_{11}e^{2i\delta_{11}} - \eta_{13}e^{2i\delta_{13}}\right|^2 \sin^2\theta\right\}, \quad (1)$$

and the inelastic cross section as

$$\sigma_{inel} = \frac{\pi}{k^2}\left[(1-\eta_1^2) + (1-\eta_{11}^2) + 2(1-\eta_{13}^2)\right]. \quad (2)$$

Here $\alpha = \frac{e^2}{\hbar v_{rel}}$,

θ is the c.m. scattering angle, $\hbar k$ the c.m. momentum, and v_{rel} the relative velocity[10]; δ_1, δ_{11}, amd δ_{13} are the $s_{1/2}$, $p_{1/2}$, and $p_{3/2}$ $T = 1$ phase shifts, respectively, and η_1 η_{11} and η_{13} correspond to the imaginary part of these phase shifts. For simplicity we have assumed that the inelastic scattering occurs principally in one of the three scattering amplitudes. Solutions for the phase shifts were obtained by setting two of the absorbitive amplitudes η, equal to unity and obtaining the third one from (2). The solutions are rather insensitive as to which phase shift was chosen as complex. In Table I and Fig. 3 we give the solutions corresponding to $\eta_1 = 0.92 \pm 0.2$ and $\eta_{11} = \eta_{13} \equiv 1$.

The results of the phase-shift analyses are given in Table I. There are three sets of phase-shift solutions.

Set A: A dominant s-wave solution. The sign of the $s_{1/2}$ phase shift can be seen to be most probably negative in agreement with earlier results at lower energy.[4,11]

Set B: A dominant $p_{1/2}$ solution which is the Minami ambiguity corresponding to set A. A unique determination of the sign of δ_{11} from our data is not possible because Coulomb interference here occurs at smaller angles than for solution A.

Set C: A combination of $p_{1/2}$ and $p_{3/2}$ amplitudes such as to reproduce near isotropy with an ambiguity in sign. This is the Fermi Yang ambiguity corresponding to solution B. If we consider the evidence for a repulsive (i.e., positive) nuclear potential from the emulsion data (2, 11) whose largest contribution comes from the forward scattering amplitude in the $T = 1$ state; vis. $V \sim -\mathrm{Re}[.75\, f_1(0) + .25\, f_0(0)]$ we can infer the sign of the dominant phase shifts. For reasonable values of $f_0(0)$ this would rule out solutions A^+, B^+ and C^+.

It should be noted here that for the dominant s-wave and $p_{1/2}$-wave solutions corresponding sets were obtained at 225 Mev.[3]

Isotropy and little variation of the scattering cross section dominate the K^+- p interaction throughout the energy interval up to 455 Mev. To ascribe the scattering to predominant repulsive s-wave interaction even at 455 Mev (Set A^-) does imply an anomalously low p-wave interaction. A $p_{1/2}$ solution (Minami ambiguity) can clearly fit an isotropic distribution at any energy. The near constancy of the cross section, however, over the large energy interval makes a dominant $p_{1/2}$ (Set B) or $p_{1/2}$ - $p_{3/2}$ mixture (Set C) solution rather unlikely. At this point we would like to emphasize that we have not explored combinations of s, p, and d waves, which will of course also reproduce the K^+ - p scattering process. As is well known from the proton-proton interaction, certain combinations of several angular momentum states can reproduce isotropic and energy-independent differential cross sections over appreciable energy intervals.

As can be seen from the inset in Fig. 3, a precise measurement of the scattering at small angles can distinguish between dominant s and dominant p solutions because of the difference in the respective Coulomb interference. Similarly, polarization measurements of the recoil proton could determine the presence of a mixture of $p_{1/2}$ and $p_{3/2}$ amplitudes or possibly higher partial waves. Scattering in the $s_{1/2}$ and in the pure $p_{1/2}$ states, respectively, does not give rise to polarization.

Inelastic interactions of positive K mesons with single pion production can proceed via three possible channels. Among the 192 inelastic scatterings recorded in the chamber, we observed examples of all three modes of pion production. Table II summarizes the results.

Those examples of Reaction I with subsequent K_1^0 decay are readily identifiable; 25 were observed. For a K_1^0 branching of 2/3 into charged pions, these events should represent 1/3 of all K^0 mesons produced in Reaction I. If all ambiguous inelastic scatterings belong to channel Ib, the observed ratio is consistent with that expected. In any event it is clear that Reaction I dominates strongly. It is interesting to note that if the K and π mesons were produced in a total isotopic spin state of $T = 1/2$, the ratio of the rates of Reactions I, II, and III would be 2:1:0, while production of the π meson and nucleon in the $T = 3/2$ state would yield at ratio 9:2:1. The data are suggestive of a dynamical effect which may be due to an enchancement in the production in one of these isotopic spin states.

We wish to thank Professor Luis W. Alvarez and many members of his group for making the 15-inch bubble chamber and analyzing facilities available to us. We are very grateful for the tireless efforts of the bubble chamber crew and the Bevatron crew as well as our own scanning and measuring group, without whose assistance this experiment would not have been possible. We would also like to acknowledge the important contributions of Mr. Thomas O'Halloran, and Dr. Wonyong Lee.

FOOTNOTES AND REFERENCES

*This work was done under the auspices of the U. S. Atomic Energy Commission.

1. W. Chinowsky, G. Goldhaber, S. Goldhaber, W. Lee, T. O'Halloran, T. F. Stubbs, W. Slater, D. H. Stork, and H. K. Ticho, in Proceedings of the International Conference on High Energy Physics at Rochester, 1960, (Interscience Publishers, New York, 1961), p. 451.

2. See for instance, J. E. Lannutti, G. Goldhaber, S. Goldhaber, W. W. Chupp, S. Giambuzzi, C. Marchi, G. Quareni, and A. Wataghin, Phys. Rev. 109, 2121 (1958); D. Keefe, A. Kernan, A. Montwill, M. Grilli, L. Guerriero, and G. A. Salandin, Nuovo cimento 12, 241 (1959).

3. D. I. Meyer, M. L. Perl, and D. A. Glaser, Phys. Rev. 107, 279 (1957).

4. T. F. Kycia, L. T. Kerth, and R. G. Baender, Phys. Rev. 118, 553 (1960).

5. H. C. Burrowes, D. O. Caldwell, D. H. Frisch, D. A. Hill, D. M. Ritson, and R. A. Schluter, Phys. Rev. Letters 2, 117 (1959).

6. G. Von Dardel, D. H. Frisch, R. Mermod, R. H. Milburn, P. A. Piroue, M. Vivargent, G. Weber, and K. Winter, Phys. Rev. Letters 5, 333 (1960).

7. We have used unpublished data of Peter Newcomb and Wilson F. Powell (Lawrence Radiation Laboratory), on π^+ interactions at 740 Mev/c, it being assumed that this angular distribution is not significantly different from that at 812 Mev/c. These data indicate an inelastic cross section approximately 25% of the total. We are grateful to the above authors for permission to use their data in advance of publication.

8. This number is a weighted average of results quoted by L. B. Okun, Annual Review of Nuclear Science 9, 61 (1959), and our own measurements on stopping K^+ mesons. In both cases the branching ratio obtained for these decay modes was $b_1 = 0.061 \pm 0.003$.

9. The uncertainty in the path length by this method comes from the reproducibility of the count, the determination of the contamination, and the statistics of the number of tracks.

10. Here $v_{rel} = v_{lab}$ of the K meson. This is essentially the relativistic form given by F. Solmitz [Phys. Rev. 94, 1799 (1954)] in the small-angle region.

11. See for instance, G. Igo, D. G. Ravenhall, J. J. Tiemann, W. W. Chupp, G. Goldhaber, S. Goldhaber, J. E. Lannutti, and R. M. Thaler, Phys. Rev. 109, 2133 (1958); M. A. Melkanoff, O. R. Price, D. H. Stork, and H. K. Ticho, Phys. Rev. 113, 1303 (1959); B. Sechi-Zorn and G. T. Zorn, Phys. Rev. 120, 1898 (1960).

12. P. Eberhard, M. Good, and H. K. Ticho, Rev. Sci. Instr. 31, 1054 (1960).

13. G. Goldhaber, S. Goldhaber, J. Kadyk, T. Stubbs, D. H. Stork, and H. K. Ticho, Separated K^+ Beam" Lawrence Radiation Laboratory Internal Report Bev-483, Feb. 26, 1960 (unpublished).

Table I. Phase shifts for K^+-Nucleon scattering at 455 Mev in the T = 1 state[a]

	Phase shifts (deg)			Probability from a χ^2 Fit	σ_{el}[b] (mb)
Solution	δ_1	δ_{11}	δ_{13}		
A^-	-47 ± 1	0.5 ± 4.5	1.5 ± 2.5	.15	12.2 ± 0.4
A^+	49 ± 1	-0.5 ± 4	0 ± 2	.01	13.0 ± 0.4
B^-	4.5 ± 2	-45.5 ± 1	-2.5 ± 1	.92	12.6 ± 0.5
B^+	-1.5 ± 1.5	46.5 ± 1	4 ± 1	.73	13.0 ± 0.5
C^-	4.5 ± 2	14.5 ± 1.5	-28 ± 1	.92	12.5 ± 0.5
C^+	-1.5 ± 2	-13.5 ± 1.5	29 ± 1	.73	13.0 ± 0.5

(a) The solutions given here are computed for $\eta_1 = 0.92$ $\eta_{11} = \eta_{13} \equiv 1$. If we value $\eta_{11} = 0.92$ and $\eta_1 = \eta_{13} \equiv 11$ for example Solution A^- becomes $\delta_1 = -45^\circ$ $\delta_{11} = 3.5^\circ$, $\delta_{13} = 1.5^\circ$.

(b) This is the nuclear elastic cross section computed from the respective phase shifts leaving out the Coulomb terms. The errors reflect the errors on the respective phase shifts.

Inelastic interactions of positive K mesons with single pion production can proceed via three possible channels. Among the 102 inelastic scatters recorded in the chamber, we observed examples of all three modes of pion production. Table II summarizes the results.

Table II. Pion Production in K^+-p Collisions

Channel	Number of Events
I (a) $K^+ + p \to K_1^0 + \pi^+ + p$, $K_1^0 \to \pi^+ + \pi^-$	25
(b) $K^+ + p \to K^0 + \pi^+ + p$, $K^0 \to K_2^0$ or neutral decay of K_1^0	35
II $K^+ + p \to K^+ + \pi^0 + p$	24
III $K^+ + p \to K^+ + \pi^+ + n$	8
Ambiguous - Ib or III	10
Total[(a)]	102

[(a)] Included in this number are nine events also consistent with π-p inelastic scatterings.

FIGURE CAPTIONS

Fig. 1. Layout of the separated K^+ beam. The beam design was similar to a separated K^- beam designed earlier (Ref. 12), and is described in detail in Ref. 13. The K^+ beam from the target (T) is focused by the quadrupole Q_1 onto slit S_1. The momentum selection is effected by bending magnet BM_1, and the subsequent mass separation by the crossed electric and magnetic field in spectrometer Sp_1. The second state is essentially a mirror image of the first. The steering magnet SM was introduced for additional freedom in the horizontal plane. C_{horiz} and C_{vert} are horizontal and vertical collimators respectively.

Fig. 2. Mass analysis of particles emerging from slot S_1 in Fig. 1. This curve was obtained by setting spectrometer Sp_1 to transmit K mesons and varying the magnetic field in spectrometer Sp_2. One thus obtains a mass analysis of particles leaving slit S_1. The final operating conditions for Sp_2 are indicated by the arrow.

Fig. 3. The $K^+ + H$ elastic differential cross section at 455 Mev. The results correspond to 1320 scattering events. The curves are computed from the various "best fit" phase shifts as given in Table 1. Sets B^-, C^-, and B^+C^+ give essentially identical differential cross section curves. For clarity, only Set A^- and Set B^- & C^- are shown in the main figure. The inset shows the small-angle behavior of all the phase-shift solutions.

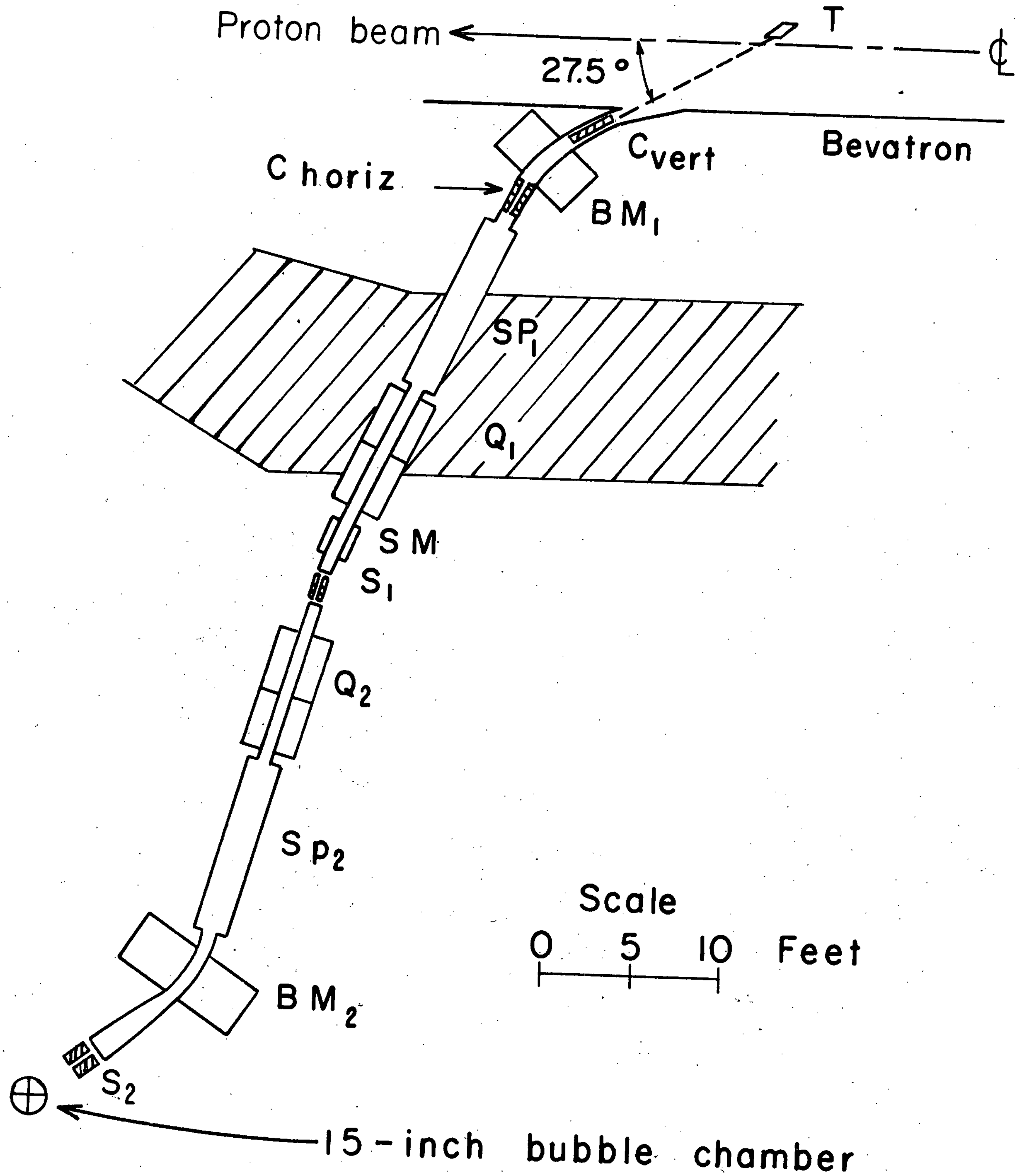

Proton beam
T
27.5°
℄
Bevatron
C vert
C horiz
B M1
SP1
Q1
S M
S1
Q2
Sp2
Scale
0 5 10 Feet
B M2
S2
15-inch bubble chamber

60238-1

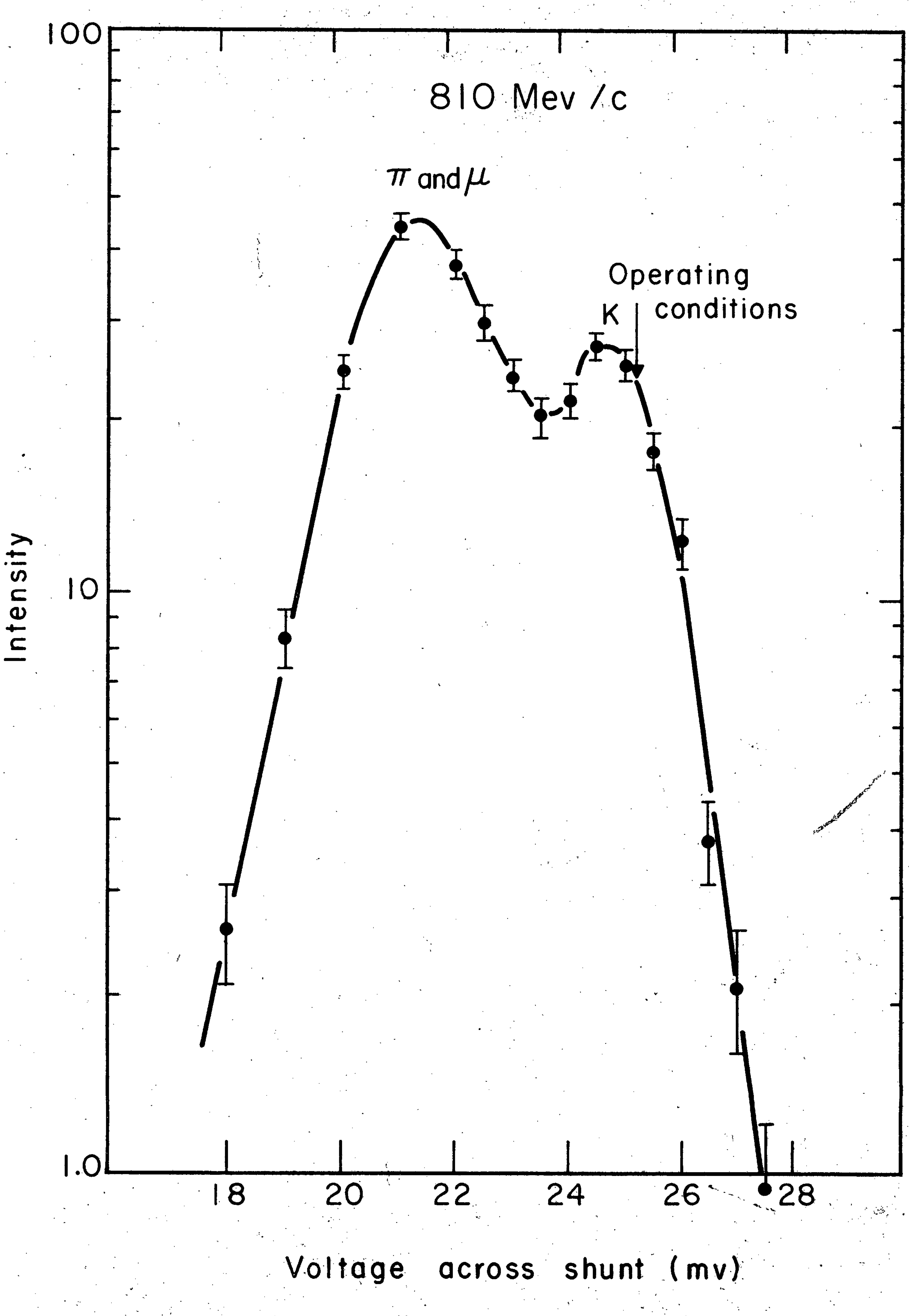
810 Mev /c
π and μ
K
Operating conditions
Intensity
100
10
1.0
18
20
22
24
26
28
Voltage across shunt (mv)
59 593-2

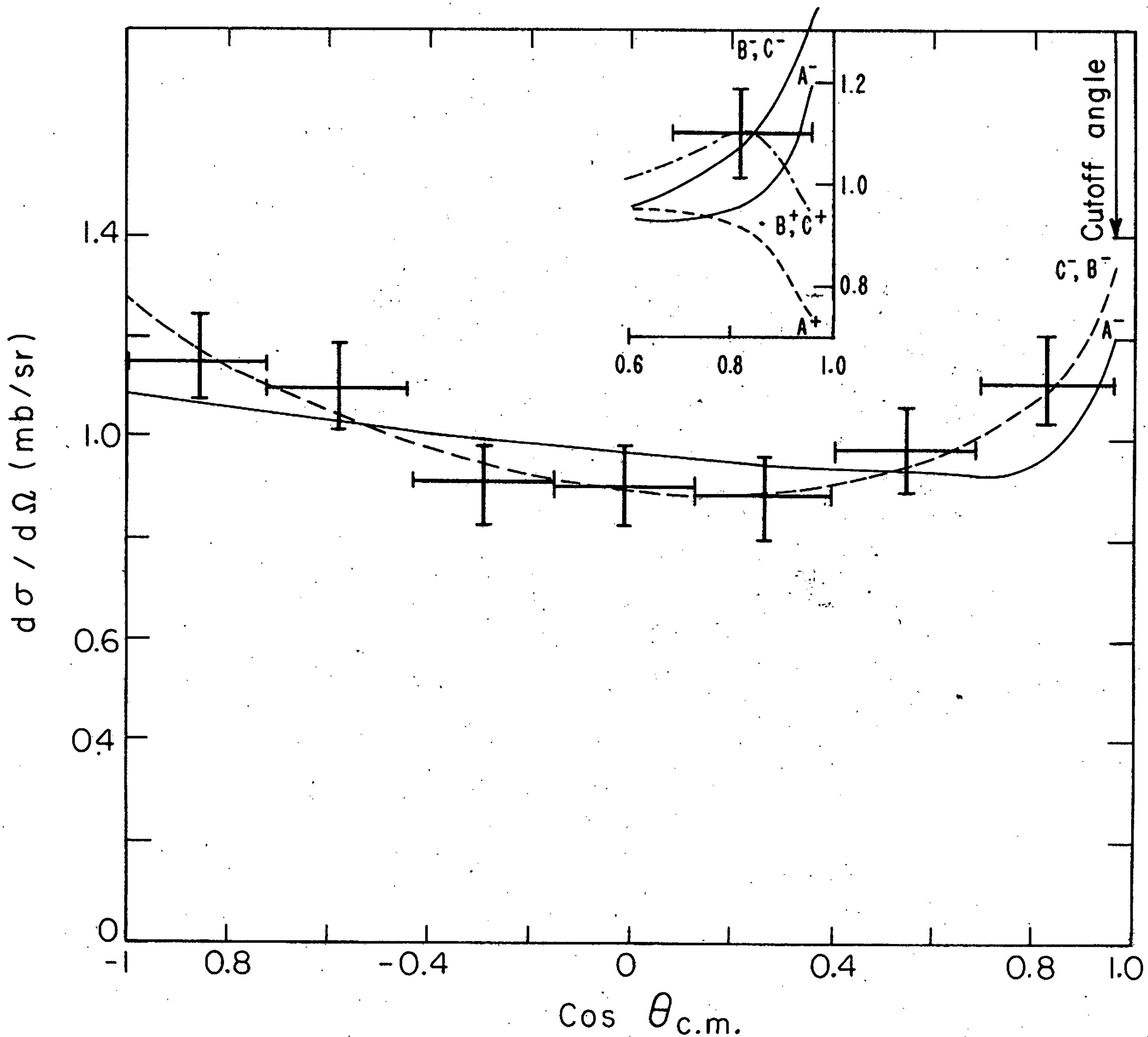
dσ / dΩ (mb/sr)
Cos θc.m.
0
0.4
0.6
1.0
1.4
-1
0.8
-0.4
0
0.4
0.8
1.0
Cutoff angle
C⁻, B⁻
A⁻
B⁻, C⁻
A⁻
B⁺, C⁺
A⁺
1.2
1.0
0.8
0.6
0.8
1.0

Fig 3
-0234-1